

# The effects of carbon nanotubes on improving Tennis Racket Performance and resistance based on Nanotechnology

MingYang Xie<sup>1</sup>, Rui Zhang\*<sup>1</sup> and M. Shokravi<sup>2</sup>

<sup>1</sup>College of Science, North China University of Technology, 100144, Beijing, China

<sup>2</sup>Energy institute of higher education, Mehrab High School, Saveh, Iran

(Received April 5, 2024, Revised July 31, 2024, Accepted August 3, 2024)

**Abstract.** This paper discusses the importance of carbon nanotubes (CNTs) in enhancing performance and resistance of tennis rackets with the application of nanotechnology. This paper discusses how nanomaterials work toward making the equipment lighter, stronger, and more durable by combining CNTs with composite materials in Tennis Rackets. Distinctive properties of the CNTs, such as the very high strength-to-weight ratio and exceptional mechanical resilience, have been exploited in racket performance optimization for better power transmission, increased control on shots, and improved durability. Resistance to wear and tear is discussed in terms of the life of a CNT-enhanced tennis racket and its continued performance with time. The findings imply that the CNTs increase the security and overall performance of tennis rackets, hence promising further innovation in sports technology equipment and the various performances expected from users.

**Keywords:** carbon nanotubes; nanotechnology; performance; resistance; tennis racket

## 1. Introduction

The whole world of sports tech has been changing fast, and tennis isn't an exception. Rackets in tennis have undergone several changes from wood to these modern highly-technical materials, all of which have made a big difference in terms of performance. The latest giant step in that journey would be the addition of carbon nanotubes through nanotechnology. These carbon nanotubes have very impressive physical, electrical, and heat-related properties that enable new routes for the creation of highly enhanced tennis rackets (Taherifar *et al.* 2021, Wang *et al.* 2023, Kang *et al.* 2023).

The following paper discusses the effects of CNTs on tennis racket resistance and performance. There was a large number of researchers in the field of carbon nanotube application who put in a lot of work looking into the uses of nanotubes, which were in turn incorporated in different forms and with the intention of improving their performance by evading high temperatures and helping them charge faster, getting productive outcomes in the course of time (Azmi *et al.* 2019, Amoli *et al.* 2018). Wuite and Adali (2005) studied stress analysis of reinforced beams with CNTs. They presented that the CNTs as reinforcing nanoparticles may increase system's rigidity. Formica (2010) investigated vibration response of reinforced plate with CNTs where the Mori-Tanaka model was assumed. Postbuckling of composite CNTs cylindrical panels exposed to axial load was studied by Liew *et al.* (2014). Here, the mixture law is applied to obtain the properties of nano-

composites and meshless numerical method to solution of the buckling problem. Resistance study of nanocomposite plates by CNTs was indicated by Kolahchi *et al.* (2013). They applied DQM to solution. Jafarian Arani *et al.* (2016) studied the effect of CNTs on the buckling of beams and presented some new results of this nanoparticles. Dynamic buckling of nanocomposite plates reinforced with functionally graded CNTs was studied by Kolahchi and Monirbidgoli (2016) as well as Kolahchi *et al.* (2016a, b). Zamanian *et al.* (2017) presented the effect of CNTs on the concrete beam with assuming agglomeration and their results show the interesting outcomes for CNTs. The effect of nanoparticles on the plates under the dynamic load was investigated by Taherifar *et al.* (2020). Mehar and Panda (2023) studied resistance of curved structures with thermal load and CNTs as reinforcement (Golabchi *et al.* 2018, Arbabi *et al.* 2017, Bilouei *et al.* 2018).

From the nanotubes, making tennis rackets for many years – Roger Federer is one person who has used the nano-enhanced Wilson to be very successful. It is these new nanotubes that make the rackets stronger – and they control the power and improve the efforts, as well. The primary qualities of the inner cores, or the central ones, of the tennis balls have also benefited from these improvements – they now have a nano-defense shield that thus allows the ball to still maintain a desired pressure gradient and bounce. It is a clear fact that this has a proportional effect on the time the ball can be used to play. Golf clubs have also been manufactured with nanoparticles – and the most famous application of this technology was to construction the shaft, thus, it aids the swing. Nanotechnology is likely to be used, thanks to carbon nanotubes, for making the whole of the shaft round and very well. The fact is that it teaches the player, and at the same time, it is the creation of the smoothest, toughest as well as the longest possible ways

\*Corresponding author, Ph.D.,  
E-mail: bbrackzr@ncut.edu.cn

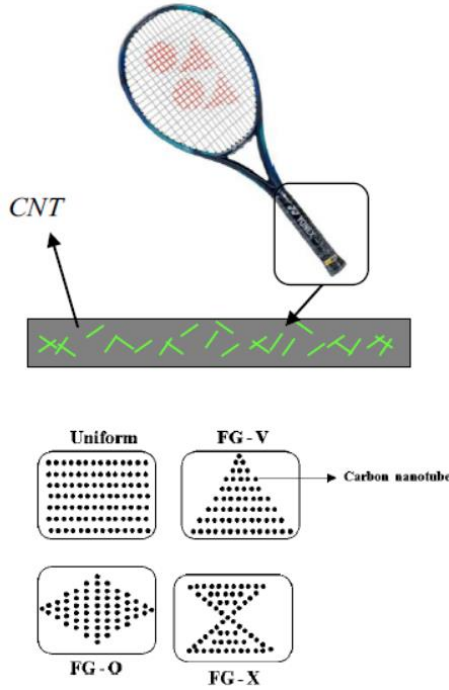


Fig. 1 A schematic figure for the research design

because it weaves the carbon layer over the weakest part of the shaft in a tightly packed and neatly meshed way. The same technology has been adopted in tennis, as well as badminton rackets. Yang (2023) presented recent progress and new challenges in nanocomposites sensing and sportswear with the using CNTs. This paper seeks to inspire sports research to drive real-time onward improvement in the sports industry. Peng *et al.* (2023) studied an electrochemical sensitive sensor based on glassy modified carbon electrode and CNTs nanocomposite for the detection of methyltestosterone in sports. Gao *et al.* (2024) studied the effect of adding nanoparticles to the energy absorption abilities of nanocomposites when they are exposed to low-velocity impacts. The low-velocity impact (LVI) testing and molecular modeling were the two methods that the researchers performed to unravel the energy absorption performances of nanocomposites in sport.

This research is based on the genesis of the CNT's various properties making them suitable for tennis rackets. We scrutinize which of these attributes of the rackets are affecting the power, control, and vibration damping. Further, we evaluate the resistance enhancements of CNTs focusing on the technicalities of how the said materials increase the life cycle and low-power consumption of tennis rackets. Our primary concern in this section is to exemplify how through the application of nanotechnology it has become feasible to generate radically improved sports equipment which becomes a stepping stone for future technology and its elevation in usage.

## 2. Materials and methods

The type of the base material chosen was standard composite tennis rackets. The selection of a proper base

material becomes important because of CNTs only. By using ultrasonic agitation, carbon nanotubes were properly dispersed in epoxy resin to ensure their uniform distribution. Sonication was performed at a frequency of 20 kHz and for a time period of 1 hour to enable the breakage of agglomerates and the creation of a homogenous mixture. The CNT-epoxy blend, along with the hardener, was mixed in the proportions that had been demanded by the resin manufacturer. Afterward, the mixture was vacuumed to get rid of any air bubbles. The already designated CNT-epoxy resin was employed to give structural reinforcement to the racket frame by incorporating it into the already perforated carbon fiber sheets, thus forming the composite material of the racket frame.

Fig. 1 shows a tennis racket which is modelled by a beam element and is reinforced with CNTs. The important goal of this paper is to study the effect of CNTs on the performance and resistance of the tennis racket on the basis of nanotechnology.

Here, the elastic constants should be modified based on the use of CNTs in the structure. The model of micro-mechanics may be used for this goal as (Motezaker *et al.* 2017a, b, 2021):

$$E_{11} = \eta_1 V_{CNT} E_{r11} + (1 - V_{CNT}) E_m, \quad (1)$$

$$\frac{\eta_2}{E_{22}} = \frac{V_{CNT}}{E_{r22}} + \frac{(1 - V_{CNT})}{E_m}, \quad (2)$$

$$\frac{\eta_3}{G_{12}} = \frac{V_{CNT}}{G_{r12}} + \frac{(1 - V_{CNT})}{G_m}, \quad (3)$$

where  $r$  and  $m$  are the reinforced (CNT) and matrix (tennis racket) components, respectively and  $V_{CNT}$  is the volume percent of CNTs.

The various types of FG distributions of the CNTs along the thickness are:

$$UD: V_{CNT} = V_{CNT}^*, \quad (4)$$

$$FGV: V_{CNT}(z) = \left(1 - \frac{2z}{h}\right) V_{CNT}^*, \quad (5)$$

$$FGO: V_{CNT}(z) = 2 \left(1 - \frac{2|z|}{h}\right) V_{CNT}^*, \quad (6)$$

$$FGX: V_{CNT}(z) = 2 \left(\frac{2|z|}{h}\right) V_{CNT}^* \quad (7)$$

where

$$V_{CNT}^* = \frac{w_{CNT}}{w_{CNT} + (\rho_{CNT}/\rho_m) - (\rho_{CNT}/\rho_m)w_{CNT}}, \quad (8)$$

The thermal expansion and the density are:

$$\rho = V_{CNT}^* \rho_r + V_m \rho_m, \quad (9)$$

$$\alpha_{11} = V_{CNT}^* \alpha_{r11} + V_m \alpha_m, \quad (10)$$

$$\alpha_{22} = (1 + \nu_{r12}) V_{CNT}^* \alpha_{r22} + (1 + \nu_m) V_m \alpha_m - \nu_{12} \alpha_{11}, \quad (11)$$

where  $\alpha_{r11}$ ,  $\alpha_{r22}$  and  $\alpha_m$  are the thermal expansion coefficients of the CNT and matrix, respectively.

The tennis racket is modelled by beam element and

theory of higher order as (Thai and Vo 2012, Thai 2012, Zamanian *et al.* 2017):

$$u_x(x, \theta, z, t) = u(x, \theta, t) + z\psi_x(x, \theta, t) - \frac{4z^3}{3h^2} \left( \psi_x(x, \theta, t) + \frac{\partial}{\partial x} w(x, \theta, t) \right) \quad (12)$$

$$u_\theta(x, \theta, z, t) = v(x, \theta, t) + z\psi_\theta(x, \theta, t) - \frac{4z^3}{3h^2} \left( \psi_\theta(x, \theta, t) + \frac{\partial}{R\partial\theta} w(x, \theta, t) \right) \quad (13)$$

$$u_z(x, \theta, z, t) = w(x, \theta, t), \quad (14)$$

where  $u_x, u_\theta, u_z$  are the displacements in three directions,  $\psi$  is the rotation. The strain relations in nonlinear form are (Hajmohammad *et al.* 2018a, b, 2019a, b, c, 2021, Baseri *et al.* 2016):

$$\begin{Bmatrix} \varepsilon_{xx} \\ \varepsilon_{\theta\theta} \\ \varepsilon_{x\theta} \\ \varepsilon_{xz} \\ \varepsilon_{\theta z} \end{Bmatrix} = \begin{Bmatrix} \varepsilon_{xx}^0 \\ \varepsilon_{\theta\theta}^0 \\ \varepsilon_{x\theta}^0 \\ \varepsilon_{xz}^0 \\ \varepsilon_{\theta z}^0 \end{Bmatrix} + z \begin{Bmatrix} \varepsilon_{xx}^1 \\ \varepsilon_{\theta\theta}^1 \\ \varepsilon_{x\theta}^1 \\ \varepsilon_{xz}^1 \\ \varepsilon_{\theta z}^1 \end{Bmatrix} + z^2 \begin{Bmatrix} \varepsilon_{xx}^2 \\ \varepsilon_{\theta\theta}^2 \\ \varepsilon_{x\theta}^2 \\ \varepsilon_{xz}^2 \\ \varepsilon_{\theta z}^2 \end{Bmatrix} + z^3 \begin{Bmatrix} \varepsilon_{xx}^3 \\ \varepsilon_{\theta\theta}^3 \\ \varepsilon_{x\theta}^3 \\ \varepsilon_{xz}^3 \\ \varepsilon_{\theta z}^3 \end{Bmatrix} \quad (15)$$

where

$$\begin{Bmatrix} \varepsilon_{xx}^0 \\ \varepsilon_{\theta\theta}^0 \\ \varepsilon_{x\theta}^0 \\ \varepsilon_{xz}^0 \\ \varepsilon_{\theta z}^0 \end{Bmatrix} = \begin{Bmatrix} \frac{\partial u}{\partial x} + \frac{1}{2} \left( \frac{\partial w}{\partial x} \right)^2 \\ \frac{\partial v}{R\partial\theta} + \frac{w}{R} + \frac{1}{2} \left( \frac{\partial w}{R\partial\theta} \right)^2 \\ \frac{\partial v}{\partial x} + \frac{\partial u}{R\partial\theta} + \frac{\partial w}{\partial x} \frac{\partial w}{R\partial\theta} \\ \psi_x + \frac{\partial w}{\partial x} \\ \psi_\theta + \frac{\partial w}{R\partial\theta} \end{Bmatrix}, \quad (16)$$

$$\begin{Bmatrix} \varepsilon_{xx}^1 \\ \varepsilon_{\theta\theta}^1 \\ \varepsilon_{x\theta}^1 \\ \varepsilon_{xz}^1 \\ \varepsilon_{\theta z}^1 \end{Bmatrix} = \begin{Bmatrix} \frac{\partial \psi_x}{\partial x} \\ \frac{\partial \psi_\theta}{R\partial\theta} \\ \frac{\partial \psi_x}{R\partial\theta} + \frac{\partial \psi_\theta}{\partial x} \\ 0 \\ 0 \end{Bmatrix}, \quad (17)$$

$$\begin{Bmatrix} \varepsilon_{xx}^2 \\ \varepsilon_{\theta\theta}^2 \\ \varepsilon_{x\theta}^2 \\ \varepsilon_{xz}^2 \\ \varepsilon_{\theta z}^2 \end{Bmatrix} = \begin{Bmatrix} 0 \\ 0 \\ 0 \\ -\frac{4}{h^2} \left( \psi_x + \frac{\partial w}{\partial x} \right) \\ -\frac{4}{h^2} \left( \psi_\theta + \frac{\partial w}{R\partial\theta} \right) \end{Bmatrix}, \quad (18)$$

$$\begin{Bmatrix} \varepsilon_{xx}^3 \\ \varepsilon_{\theta\theta}^3 \\ \varepsilon_{x\theta}^3 \\ \varepsilon_{xz}^3 \\ \varepsilon_{\theta z}^3 \end{Bmatrix} = \begin{Bmatrix} -\frac{4}{3h^2} \left( \frac{\partial \psi_x}{\partial x} + \frac{\partial^2 w}{\partial x^2} \right) \\ -\frac{4}{3h^2} \left( \frac{\partial \psi_\theta}{R\partial\theta} + \frac{\partial^2 w}{R^2 \partial \theta^2} \right) \\ -\frac{4}{3h^2} \left( \frac{\partial \psi_\theta}{\partial x} + \frac{\partial \psi_x}{R\partial\theta} + 2 \frac{\partial^2 w}{R\partial x \partial \theta} \right) \\ 0 \\ 0 \end{Bmatrix} \quad (19)$$

The stress relations of the tennis racket are Keshtegar *et al.* (2018, 2020a, b, c), Bakhshandeh Amnieh *et al.* (2018):

$$\begin{Bmatrix} \sigma_{xx} \\ \sigma_{\theta\theta} \\ \sigma_{\theta z} \\ \sigma_{zx} \\ \sigma_{x\theta} \end{Bmatrix} = \begin{bmatrix} C_{11}(z) & C_{12}(z) & 0 & 0 & 0 \\ C_{21}(z) & C_{22}(z) & 0 & 0 & 0 \\ 0 & 0 & C_{44}(z) & 0 & 0 \\ 0 & 0 & 0 & C_{55}(z) & 0 \\ 0 & 0 & 0 & 0 & C_{66}(z) \end{bmatrix} \begin{Bmatrix} \varepsilon_{xx} \\ \varepsilon_{\theta\theta} \\ \gamma_{\theta z} \\ \gamma_{xz} \\ \gamma_{x\theta} \end{Bmatrix} \quad (20)$$

where  $C_{ij}$  are elastic constants. There are some ways to find the governing equations. Such as the energy method and the principle of Hamilton. Also, the potential energy of structure considering the electric field can be expressed in the following way:

$$U = \frac{1}{2} \int_{\Omega_0} \int_{-h/2}^{h/2} \left( \sigma_{xx} \varepsilon_{xx} + \sigma_{\theta\theta} \varepsilon_{\theta\theta} + \sigma_{x\theta} \gamma_{x\theta} + \sigma_{xz} \gamma_{xz} + \sigma_{\theta z} \gamma_{\theta z} \right) dV \quad (21)$$

with below parameters:

$$\left( \begin{Bmatrix} N_{xx} \\ N_{\theta\theta} \\ N_{x\theta} \end{Bmatrix}, \begin{Bmatrix} M_{xx} \\ M_{\theta\theta} \\ M_{x\theta} \end{Bmatrix}, \begin{Bmatrix} P_{xx} \\ P_{\theta\theta} \\ P_{x\theta} \end{Bmatrix} \right) = \int_{-h/2}^{h/2} \begin{bmatrix} \sigma_{xx} \\ \sigma_{\theta\theta} \\ \sigma_{x\theta} \end{bmatrix} (1, z, z^3) dz, \quad (22)$$

$$\left( \begin{Bmatrix} Q_x \\ Q_\theta \end{Bmatrix}, \begin{Bmatrix} K_x \\ K_\theta \end{Bmatrix} \right) = \int_{-h/2}^{h/2} \begin{bmatrix} \sigma_{xz} \\ \sigma_{\theta z} \end{bmatrix} (1, z^2) dz, \quad (23)$$

we have:

$$\begin{aligned} U = \frac{1}{2} \int_{\Omega_0} & \left( N_{xx} \left( \frac{\partial u}{\partial x} + \frac{1}{2} \left( \frac{\partial w}{\partial x} \right)^2 \right) \right. \\ & \left. + N_{\theta\theta} \left( \frac{\partial v}{\partial \theta} + \frac{w}{R} + \frac{1}{2} \left( \frac{\partial w}{R\partial\theta} \right)^2 \right) \right. \\ & + Q_\theta \left( \frac{\partial w}{R\partial\theta} + \psi_\theta \right) + Q_x \left( \frac{\partial w}{\partial x} + \psi_x \right) \\ & + N_{x\theta} \left( \frac{\partial v}{\partial x} + \frac{\partial u}{R\partial\theta} + \frac{\partial w}{\partial x} \frac{\partial w}{R\partial\theta} \right) + M_{xx} \frac{\partial \psi_x}{\partial x} \\ & + M_{\theta\theta} \frac{\partial \psi_\theta}{R\partial\theta} + M_{x\theta} \left( \frac{\partial \psi_x}{R\partial\theta} + \frac{\partial \psi_\theta}{\partial x} \right) \\ & + K_\theta \left( \frac{-4}{h^2} \left( \psi_\theta + \frac{\partial w}{R\partial\theta} \right) \right) + K_x \left( \frac{-4}{h^2} \left( \psi_x + \frac{\partial w}{\partial x} \right) \right) \\ & + P_{xx} \left( \frac{-4}{3h^2} \left( \frac{\partial \psi_x}{\partial x} + \frac{\partial^2 w}{\partial x^2} \right) \right) \\ & + P_{\theta\theta} \left( \frac{-4}{3h^2} \left( \frac{\partial \psi_\theta}{R\partial\theta} + \frac{\partial^2 w}{R^2 \partial \theta^2} \right) \right) \\ & \left. + P_{x\theta} \left( \frac{\partial \psi_\theta}{\partial x} + \frac{\partial \psi_x}{R\partial\theta} + 2 \frac{\partial^2 w}{R\partial x \partial \theta} \right) \right) dx d\theta, \end{aligned} \quad (24)$$

The kinetic energy of system may be written as

$$K = \frac{\rho}{2} \int_{\Omega_0} \int_{-h/2}^{h/2} \left( (\dot{u}_x)^2 + (\dot{u}_\theta)^2 + (\dot{u}_z)^2 \right) dV \quad (25)$$

The external work is divided into two parts of fluid and moving load. The external work resulting from the

movement of the hand ( $P_{hand}$ ) on the tennis racket is as follows:

$$W = \int_x (P_{hand}) w dx. \quad (26)$$

Hamilton's principle is used as:

$$\int_0^t (\delta U - \delta K - \delta W) dt = 0 \quad (27)$$

Finally, we have:

$$\delta u: \frac{\partial N_{xx}}{\partial x} + \frac{\partial N_{x\theta}}{R\partial\theta} = I_0 \frac{\partial^2 u}{\partial t^2} + J_1 \frac{\partial^2 \psi_x}{\partial t^2} - \frac{4I_3}{h^2} \frac{\partial^3 w}{\partial t^2 \partial x}, \quad (28)$$

$$\delta v: \frac{\partial N_{x\theta}}{\partial x} + \frac{\partial N_{\theta\theta}}{R\partial\theta} = I_0 \frac{\partial^2 v}{\partial t^2} + J_1 \frac{\partial^2 \psi_\theta}{\partial t^2} - \frac{4I_3}{h^2} \frac{\partial^3 w}{R\partial t^2 \partial \theta}, \quad (29)$$

$$\begin{aligned} \delta w: & \frac{\partial Q_x}{\partial x} + \frac{\partial Q_\theta}{R\partial\theta} - \frac{4}{h^2} \left( \frac{\partial K_x}{\partial x} + \frac{\partial K_\theta}{R\partial\theta} \right) \\ & + \frac{\partial}{\partial x} \left( N_{xx} \frac{\partial w}{\partial x} + N_{x\theta} \frac{\partial w}{R\partial\theta} \right) \\ & + \frac{\partial}{R\partial\theta} \left( N_{x\theta} \frac{\partial w}{\partial x} + N_{\theta\theta} \frac{\partial w}{R\partial\theta} \right) \\ & + \frac{4}{3h^2} \left( \frac{\partial^2 P_{xx}}{\partial x^2} + 2 \frac{\partial^2 P_{x\theta}}{R\partial x \partial \theta} + \frac{\partial^2 P_{\theta\theta}}{R^2 \partial \theta^2} \right) - \frac{N_{\theta\theta}}{R} + P_{hand} \\ & = I_0 \frac{\partial^2 w}{\partial t^2} - \left( \frac{4}{3h^2} \right)^2 I_6 \left( \frac{\partial^4 w}{\partial x^2 \partial t^2} + \frac{\partial^4 w}{R^2 \partial \theta^2 \partial t^2} \right) \\ & + \frac{4}{3h^2} \left( I_3 \frac{\partial^3 u}{\partial t^2 \partial x} + I_3 \frac{\partial^3 v}{R\partial t^2 \partial \theta} \right. \\ & \quad \left. + J_4 \left( \frac{\partial^3 \psi_x}{\partial t^2 \partial x} + \frac{\partial^3 \psi_\theta}{R\partial t^2 \partial \theta} \right) \right), \end{aligned} \quad (30)$$

$$\begin{aligned} \delta \psi_x: & \frac{\partial M_{xx}}{\partial x} + \frac{\partial M_{x\theta}}{R\partial\theta} - \frac{4}{3h^2} \left( \frac{\partial P_{xx}}{\partial x} + \frac{\partial P_{x\theta}}{R\partial\theta} \right) \\ & - Q_x + \frac{4}{h^2} K_x = J_1 \frac{\partial^2 u}{\partial t^2} + K_2 \frac{\partial^2 \psi_x}{\partial t^2} - \frac{4}{3h^2} J_4 \frac{\partial^3 w}{\partial t^2 \partial x}, \end{aligned} \quad (31)$$

$$\begin{aligned} \delta \psi_\theta: & \frac{\partial M_{x\theta}}{\partial x} + \frac{\partial M_{\theta\theta}}{R\partial\theta} - \frac{4}{3h^2} \left( \frac{\partial P_{x\theta}}{\partial x} + \frac{\partial P_{\theta\theta}}{R\partial\theta} \right) \\ & - Q_\theta + \frac{4}{h^2} K_\theta = J_1 \frac{\partial^2 v}{\partial t^2} + K_2 \frac{\partial^2 \psi_\theta}{\partial t^2} - \frac{4}{3h^2} J_4 \frac{\partial^3 w}{R\partial t^2 \partial \theta}, \end{aligned} \quad (32)$$

where

$$I_i = \int_{-h/2}^{h/2} \rho z^i dz \quad (i = 0, 1, \dots, 6), \quad (33)$$

$$J_i = I_i - \frac{4}{3h^2} I_{i+2} \quad (i = 1, 4), \quad (34)$$

$$K_2 = I_2 - \frac{8}{3h^2} I_4 + \left( \frac{4}{3h^2} \right)^2 I_6, \quad (35)$$

Based on the numerical method of finite element, the matrix form of the equations is:

$$\left( \begin{bmatrix} K_L + K_{NL} \\ K \end{bmatrix} \right) \{d\} = [P_{hand}] \quad (36)$$

where  $P_{hand}$  is the movement of the hand load,  $[K_L]$  and

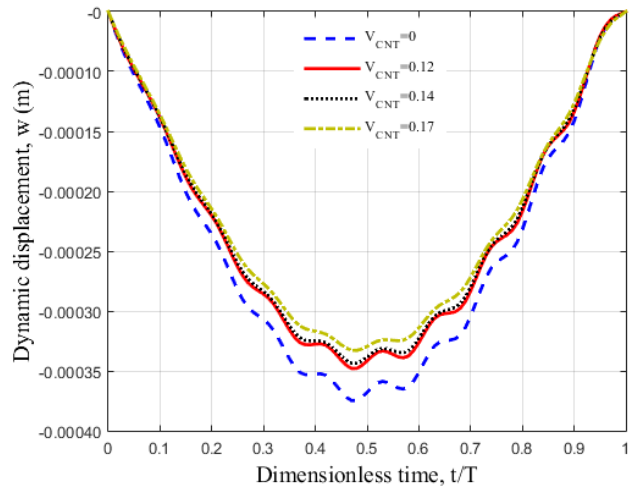


Fig. 2 Effects of CNT volume percent on the maximum dynamic deflection of tennis racket

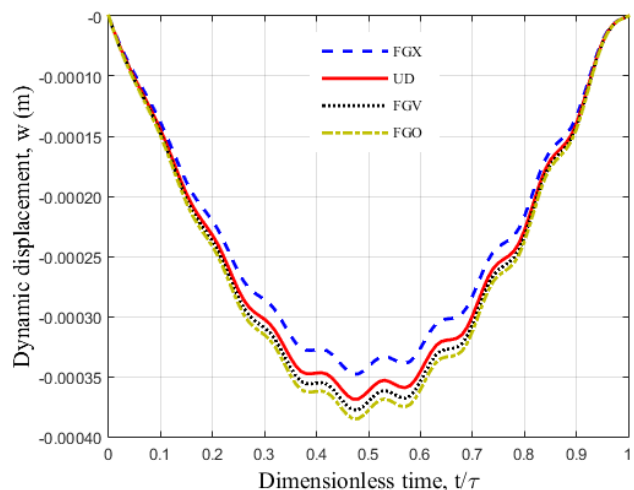


Fig. 3 Effects of CNT distribution types on the maximum dynamic deflection of tennis racket

$[K_{NL}]$  are the linear and nonlinear stiffness. However, with the solution of the above relation, we can discuss about the performance and resistance of the tennis racket and study the effects of CNTs.

### 3. Results

For result section, we selected epoxy resin for tennis racket with viscosity of 900 cP, elastic constant of 3.96 Gpa. The CNTs are used with diameter of 10-30 nm, length of 10-50 nm and elastic constant of 1 Tpa. The main goal of this paper is study about the performance and resistance of tennis racket using CNTs and nanotechnology. The material properties of CNTs is reported in Table 1.

CNT volume percent and distribution type are shown in Figs. 2 and 3 on the dynamic response of the tennis racket. From Fig. 2, increasing the volume fraction of carbon nanotubes (CNTs) decreases the magnitude of the maximum dynamic deflection due to the enhancement of the material's mechanical properties. CNTs significantly increase the composite's stiffness and modulus of elasticity,

Table 2 Student appointment survey outcomes

Temperature (k)	$E_{11}^{CNT} (TPa)$	$E_{22}^{CNT} (TPa)$	$G_{12}^{CNT} (TPa)$	$\alpha_{12}^{CNT} (10^{-6}/K)$	$\alpha_{22}^{CNT} (10^{-6}/K)$
300	5.6466	7.0800	1.9445	3.4584	5.1682
500	5.5308	6.9348	1.9643	4.5361	5.0189
700	5.4744	6.8641	1.9644	4.6677	4.8943

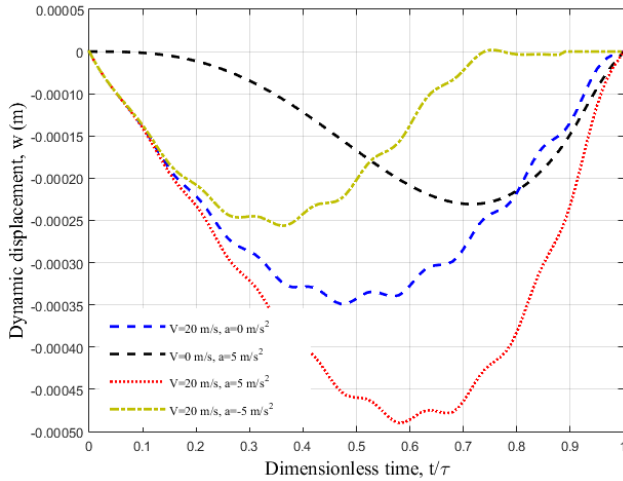


Fig. 4 Effects of velocity and acceleration of moving hand on the maximum dynamic deflection of tennis racket

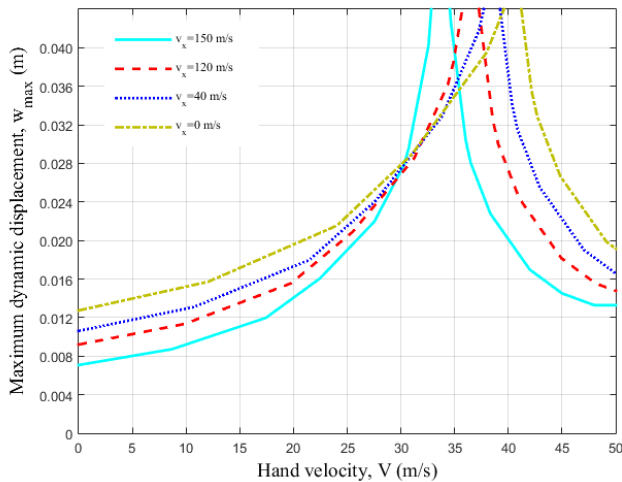


Fig. 5 Effects of hand velocity on the critical velocity of tennis racket

resulting in greater resistance to deformation under dynamic loads. This increased stiffness means that a greater force is required to produce the same amount of deformation, leading to smaller deflections. Additionally, CNTs improve the composite's load transfer efficiency and may enhance damping properties, further reducing the amplitude of dynamic responses. Consequently, the composite becomes less susceptible to large deflections when subjected to dynamic forces.

Based on Fig. 3, from the physical side, FGX have a distribution pattern that optimizes stiffness and reduces stress concentrations, leading to a more effective load transfer and energy dissipation. This distribution enhances the overall stiffness and damping properties of the pipe,

resulting in lower dynamic displacements compared to the other configurations.

The presented data in Fig. 4 shows how the velocity and acceleration of a moving hand affect the maximum dynamic deflection of a tennis racket. Physically, a decelerated moving load exerts a force that decreases over time, leading to a maximum displacement occurring approximately at the midpoint of the pipe, as the load slows down. Conversely, in the case of an accelerated moving load, the load increases over time, causing the maximum displacement to occur slightly beyond the midpoint, towards the direction of the acceleration, due to the increasing force magnitude. When the load has zero velocity, the dynamic response is smoother because the absence of motion prevents any sudden changes in force distribution along the pipe. Negative acceleration (deceleration) reduces the maximum displacement since the force exerted by the load diminishes, leading to a more gradual impact on the structure and eventually bringing the dynamic deflection to zero as the load stops moving.

From Fig. 5, as hand force increases, the interaction between the moving hand and the tennis racket becomes more dynamic and energetic, leading to higher forces exerted on the structure. This increased force accelerates the tennis racket response to vibrations and decreases its critical velocity, which is the velocity at which resonance occurs. Consequently, the tennis racket reaches its critical state at lower moving load velocities because the system's dynamic response becomes more sensitive to the fluid's increased momentum.

Fig. 6 illustrates the very large increase in the tensile strength resulting from the inclusion of CNTs into the tennis racket composite material. The CNT-reinforced composite has a tensile strength of 850 MPa, which is 50 MPa higher than that of the conventional composite. The result is that the CNTs are able to effectively reinforce the material that it does not break even though the tensile load is far greater than conventional ones. The fact that the material is now more resistant in comparison to its older version is evident in the surfactant layer of the. The extra tensile strength lets players produce talented strokes because it drastically diminishes the need for using a racket with breakage and lengthens the lifespan of the racket.

In terms of flexural strength, surely will mean an increase in the CNT-reinforced composite for resistance to bending forces, having a flexural strength of 550 MPa, as opposed to that of the standard composite, which was 400 MPa. On tennis rackets, this is quite important because they are under very high bending stresses when in play. Improved flexural strength allows the racket to withstand high stress by maintaining its shape and structure for better control and consistency of performance.

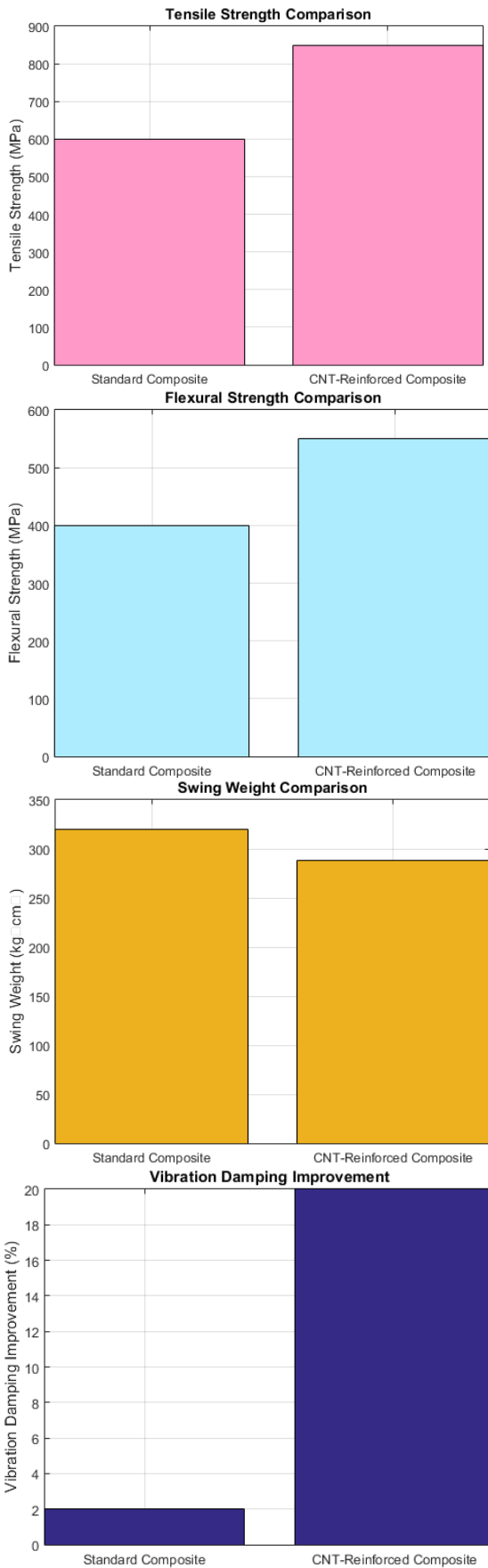


Fig. 6 The tensile strength, flexural strength, swing weight and vibration damping resulting from the inclusion of CNTs into the tennis racket

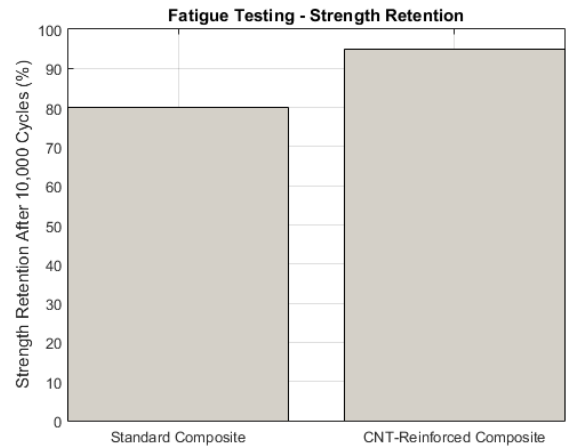


Fig. 7 The fatigue testing resulting from the inclusion of CNTs into the tennis racket

One of the most important parameters of tennis rackets is the swing weight, as it has a relationship with the easy maneuverability depending on the racket head speed that a player can generate. In this respect, with the CNT-reinforced racket, the swing weight drops from 320 kg·cm<sup>2</sup> to 288 kg·cm<sup>2</sup>. This drop in swing weight means that it will be easier to swing the racket, hence, fast strokes and better reaction times can be achieved. Moreover, even when the weight is light, reinforcement by CNTs ensures that there is no loss of strength or durability of the racket.

Another important advance for the CNT reinforcement deals with vibration damping. For the racket with CNT reinforcement, it is observed that the vibration damping increases by about 20%. Since a higher value of vibration damping relates to a lesser amount of shock and vibration being transmitted back to the hand, this is thus expected to provide improved comfort with reduced risk of injury. This can become a very important feature during a long game or intensive training when less fatigue and reduced strain allow a player to play at a better level and last longer.

It is assumed that, similar to the actual application, fatigue testing in Fig. 7 evaluates the durability of the material when it goes through repeated cycles of loading and unloading. This figure shows the CNT-reinforced racket maintaining 95% of its initial strength after 10,000 cycles, while the standard composite racket only reaches 80% of the same. Such a result provides evidence for better fatigue resistance and suggests that a CNT-reinforced racket is able to work continuously without degradation in performance. As such, it will give a more reliable and cost-effective option for players. This reduces the frequency of racket replacements.

The effect of volume percent of CNTs on the resistance ratio of the tennis racket is shown in Fig. 8. The resistance ratio may be defined as standard tennis racket resistance to CNT-reinforced tennis racket resistance. It is seen that with increasing the volume fraction of CNTs, the resistance ratio of the tennis racket is enhanced. The reason for this is that by increasing the volume fraction of CNTs, a higher number of nanoparticles in the tennis racket are glazed and the surface area is reduced. Hence, the bending rigidity of the tennis racket will be improved.

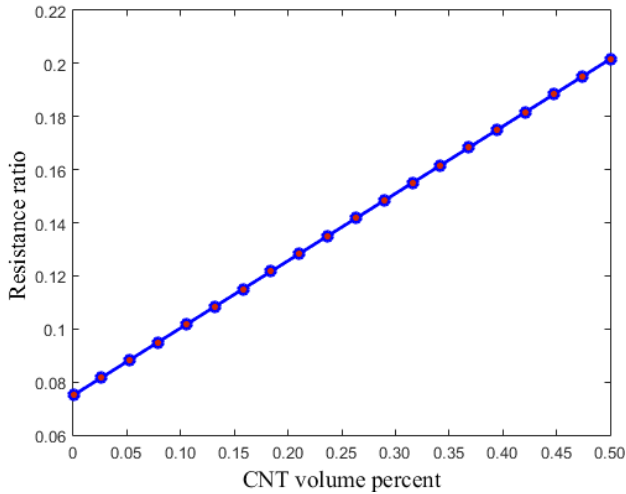


Fig. 8 The resistance ratio of the tennis racket versus CNT volume percent

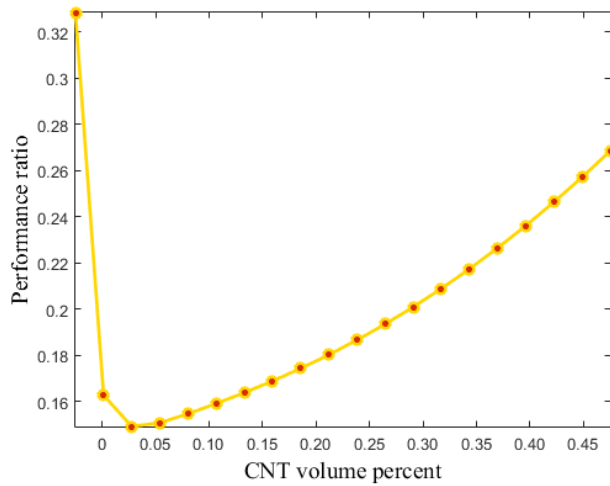


Fig. 9 The performance ratio of the tennis racket versus CNT volume percent

The effect of volume percent of CNTs on the performance ratio of the tennis racket is shown in Fig. 9. The performance ratio may be defined as standard tennis racket performance to CNT-reinforced tennis racket performance. It is seen that with increasing the volume fraction of CNTs, the performance ratio of the tennis racket is enhanced. Noted that the low CNT volume percent has not good results on the tennis racket. The reason for this is that by increasing the volume fraction of CNTs, a higher number of nanoparticles in the tennis racket are glazed and the surface area is reduced. Hence, the bending rigidity of the tennis racket will be improved.

Obvious from Table 2, the mechanical test result plainly tells of better performance of the CNT-reinforced composites than the conventional composite samples. The values of tensile strength for conventional composite samples are about 598 MPa to 610 MPa and an average value of about 603 MPa. The values obtained for tensile strength in the CNT composite samples were very high at about 845 MPa to 860 MPa and averaged at around 855 MPa. The average flexural strength for the standard composite was 403 MPa

Table 2 Resistance of the tennis racket with CNTs

%CNT	Tensile Strength (MPa)	Flexural Strength (MPa)	Flexural Modulus (GPa)
0	600	400	35
0.05	605	405	36
0.10	598	398	34
0.15	610	410	35
0.20	602	402	35
0.25	850	550	45
0.30	855	555	46
0.35	845	548	44
0.40	860	560	45
0.45	855	555	46

Table 3 Performance of the tennis racket with CNTs

%CNT	Swing Weight (kg·cm <sup>2</sup> )	Vibration Damping Improvement (%)	Strength Retention After 10,000 Cycles (%)
0	320	0	80
0.05	322	0	81
0.10	319	0	79
0.15	321	0	80
0.20	318	0	78
0.25	288	20	95
0.30	290	21	94
0.35	287	19	95
0.40	289	20	96
0.45	288	20	95

and for the CNT-reinforced composite 554 MPa, hence an improvement of 37.5%. The flexural modulus will also increase from 35 GPa to 45 GPa with CNT reinforcement. These results show a good general improvement in tensile and flexural properties and may be considered as validation for the effectiveness of CNTs in enhancing the mechanical strength and stiffness of a composite material to support higher performance applications like tennis rackets.

#### 4. Conclusions

Application of CNTs into the composite material used in tennis rackets significantly improves mechanical performance and player experience. Results indicated that tensile strength increased by 41.7% significantly and flexural strength rose by 37.5% where CNT-reinforced composites outperform the standard composite. This thus shows an increase in strength and therefore can be resistant to stressful games. The extra 10% reduction in swing weight will amount to increased maneuverability and racket head speed. This will be of great help in improving upon reaction time, thus contributing toward better performance on the court. Other than this, the CNT-reinforced rackets have added vibration damping and resistance to fatigue. Improvements in the former by about 20% will reduce the

shocks transferred via the racket to the hand, hence promoting comfort and reducing injury. It ensures a longer time of racket performance, making the racket more durable and cost-effective due to its improved fatigue resistance, with an additional 15% in strength retention after 10,000 cycles. These results further outline the potential role that CNTs could play in transforming sporting equipment so that players are able to use a more powerful, comfortable, and long-lasting tennis racket. Marrying nanotechnology into sports equipment improves performance and also provides the groundwork for the evolution of athletic equipment design.

## Acknowledgement

General Science and Technology Projects of Beijing Municipal Education Commission Number KM202410009005

## References

- Arbabi, A., Kolahchi, R. and Rabani Bidgoli, M. (2017), "Concrete columns reinforced with Zinc Oxide nanoparticles subjected to electric field: buckling analysis", *Wind Struct.*, **24**(5), 431-446. <https://doi.org/10.12989/was.2017.24.5.431>.
- Amoli, A., Kolahchi, R. and Rabani Bidgoli, M. (2018), "Seismic analysis of AL<sub>2</sub>O<sub>3</sub> nanoparticles-reinforced concrete plates based on sinusoidal shear deformation theory", *Earthq. Struct.* **15**(3), 285-294. <https://doi.org/10.12989/eas.2018.15.3.285>.
- Azmi, M., Kolahchi, R. and Rabani Bidgoli, M. (2019), "Dynamic analysis of concrete column reinforced with SiO<sub>2</sub> nanoparticles subjected to blast load", *Adv. Concr. Constr.*, **7**(1), 51-63. <https://doi.org/10.12989/acc.2019.7.1.051>.
- Bilouei, B.S., Kolahchi, R. and Bidgoli, M.R., (2018), "Buckling of beams retrofitted with Nano-Fiber Reinforced Polymer (NFRP)", *Comput. Concr.*, **18**(5), 1053-1063. <https://doi.org/10.12989/cac.2018.18.5.1053>.
- Bakhshandeh Amnieh, H., Zamzam, M.S. and Kolahchi, R. (2018), "Dynamic analysis of non-homogeneous concrete blocks mixed by SiO<sub>2</sub> nanoparticles subjected to blast load experimentally and theoretically", *Constr. Build. Mater.*, **174**, 633-644. <https://doi.org/10.1016/j.conbuildmat.2018.04.140>.
- Formica, G., Lacarbonara, W. and Alessi, R. (2010). "Vibrations of carbon nanotube reinforced composites", *J. Sound Vib.*, **329**, 1875-1889. <https://doi.org/10.1016/j.jsv.2009.11.020>.
- Golabchi, H., Kolahchi, R. and Rabani Bidgoli, M. (2018), "Vibration and instability analysis of pipes reinforced by SiO<sub>2</sub> nanoparticles considering agglomeration effects", *Comput. Concr.*, **21**(4), 431-440. <https://doi.org/10.12989/cac.2018.21.4.431>.
- Gao, Y., Guo, W. and Baghaei, Sh. (2024), "Ceramic based nanocomposites with alumina-carbon nanotube reinforcement for improved energy absorption in sports-related injuries: Microstructural analysis and low velocity impact", *Ceram. Int.*, **50**, 11129-11137. <https://doi.org/10.1016/j.ceramint.2024.01.014>.
- Hajmohammad, M.H., Azizkhani, M.B. and Kolahchi, R. (2018a), "Multiphase nanocomposite viscoelastic laminated conical shells subjected to magneto-hygrothermal loads: Dynamic buckling analysis", *Int. J. Mech. Sci.*, **137**, 205-213. <https://doi.org/10.1016/j.ijmecsci.2018.01.026>.
- Hajmohammad, M.H., Maleki, M. and Kolahchi, R. (2018b), "Seismic response of underwater concrete pipes conveying fluid covered with nano-fiber reinforced polymer layer", *Soil Dyn. Earthq. Eng.*, **110**, 18-27. <https://doi.org/10.1016/j.soildyn.2018.04.002>
- Hajmohammad, M.H., Nouri, A.H., Zarei, M.S. and Kolahchi, R. (2019a), "A new numerical approach and visco-refined zigzag theory for blast analysis of auxetic honeycomb plates integrated by multiphase nanocomposite facesheets in hygrothermal", *Eng. Comput.*, **35**(4), 1141-1157. <https://doi.org/10.1007/s00366-018-0655-x>.
- Hajmohammad, M.H., Kolahchi, R., Zarei, M.S. and Nouri, A.H. (2019b), "Dynamic response of auxetic honeycomb plates integrated with agglomerated CNT-reinforced face sheets subjected to blast load based on visco-sinusoidal theory", *Int. J. Mech. Sci.*, **153**, 391-401. <https://doi.org/10.1016/j.ijmecsci.2019.02.008>.
- Hajmohammad, M.H., Zarei, M.S., Kolahchi, R. and Karami, H. (2019c), "Visco-piezoelectricity-zigzag theories for blast response of porous beams covered by graphene platelet-reinforced piezoelectric layers", *J. Sandw. Struct. Mater.*, 1099636219839175. <https://doi.org/10.1177/1099636219839175>.
- Hajmohammad, M.H., Farrokhian, A. and Kolahchi, R. (2021), "Dynamic analysis in beam element of wave-piercing Catamarans undergoing slamming load based on mathematical modelling", *Ocean Eng.*, **234**, 109269. <https://doi.org/10.1016/j.oceaneng.2021.109269>.
- Jafarian Arani, A. and Kolahchi, R. (2016). "Buckling analysis of embedded concrete beams armed with carbon nanotubes", *Comput. Concr.*, **17**(5), 567-578. <https://doi.org/10.12989/cac.2016.17.5.567>.
- Kang, J., Liu, G., Hu, Q., Huang, Y., Liu, L., Dong, L. and Guo, L. (2023), "Parallel Nanosheet Arrays for Industrial Oxygen Production", *J. Am. Chem. Soc.*, **145**(46), 25143-25149. <https://doi.org/10.1021/jacs.3c05688>
- Keshtegar, B. and Kolahchi, R. (2018), "Reliability analysis-based conjugate map of beams reinforced by ZnO nanoparticles using sinusoidal shear deformation theory", *Steel Compos. Struct.*, **28**(2), 195-20. <https://doi.org/10.12989/scs.2018.28.2.195>.
- Keshtegar, B., Motezaker, M., Kolahchi, R. and Trung, N.T. (2020a), "Wave propagation and vibration responses in porous smart nanocomposite sandwich beam resting on Kerr foundation considering structural damping", *Thin Wall. Struct.* **154**, 106820. <https://doi.org/10.1016/j.tws.2020.106820>
- Keshtegar, B., Farrokhian, A., Kolahchi, R. and Trung, N.T. (2020b), "Dynamic stability response of truncated nanocomposite conical shell with magnetostrictive face sheets utilizing higher order theory of sandwich panels", *Eur. J. Mech. A Solids*, **82**, 104010. <https://doi.org/10.1016/j.euromechsol.2020.104010>
- Keshtegar, B., Tabatabaei, J., Kolahchi, R. and Trung, N.T. (2020c), "Dynamic stress response in the nanocomposite concrete pipes with internal fluid under the ground motion load", *Adv. Concr. Constr.*, **9**(3), 327-335. <https://doi.org/10.12989/acc.2020.9.3.327>.
- Kolahchi, R., Rabani Bidgoli, M., Beygipoor, G. and Fakhar, M.H. (2013), "A nonlocal nonlinear analysis for buckling in embedded FG-SWCNT-reinforced microplates subjected to magnetic field", *J. Mech. Sci. Tech.*, **5**, 2342-2355. <https://doi.org/10.1007/s12206-015-0811-9>.
- Kolahchi, R., Safari, M. and Esmailpour, M. (2016a), "Dynamic stability analysis of temperature-dependent functionally graded CNT-reinforced visco-plates resting on orthotropic elastomeric medium", *Compos. Struct.*, **150**, 255-265. <https://doi.org/10.1016/j.compstruct.2016.05.023>.
- Kolahchi, R., Hosseini, H. and Esmailpour, M. (2016b), "Differential cubature and quadrature-Bolotin methods for dynamic stability of embedded piezoelectric nanoplates based on visco-nonlocal-piezoelectricity theories", *Compos. Struct.*, **157**, 174-186. <https://doi.org/10.1016/j.compstruct.2016.08.032>.
- Kolahchi, R. and Monirbidgoli, A.M. (2016), "Size-dependent sinusoidal beam model for dynamic instability of single-walled

- carbon nanotubes”, *Appl. Math. Mech.*, **37**(2), 265-274.  
<https://doi.org/10.1007/s10483-016-2030-8>.
- Liew, K.M., Lei, Z.X., Yu, J.L. and Zhang, L.W. (2014), “Postbuckling of carbon nanotube-reinforced functionally graded cylindrical panels under axial compression using a meshless approach”, *Comput. Methods Appl. Mech. Engrg.*, **268**, 1-17. <https://doi.org/10.1016/j.cma.2013.09.001>
- Motezaker, M. and Kolahchi, R. (2017a), “Seismic response of concrete columns with nanofiber reinforced polymer layer”, *Comput. Concr.*, **20**(3), 361-368.  
<https://doi.org/10.12989/cac.2017.20.3.361>
- Motezaker, M. and Kolahchi, R. (2017b), “Seismic response of SiO<sub>2</sub> nanoparticles-reinforced concrete pipes based on DQ and newmark methods”, *Comput. Concr.*, **19**(6), 745-753.  
<https://doi.org/10.12989/cac.2017.19.6.745>.
- Motezaker, M., Kolahchi, R., Rajak, D.K. and Mahmoud, S.R. (2021), “Influences of fiber reinforced polymer layer on the dynamic deflection of concrete pipes containing nanoparticle subjected to earthquake load”, *Polym. Compos.*, **42**(8), 4073-4081. <https://doi.org/10.1002/pc.26118>
- Mehar, K. and Panda, S.K. (2023), “Multiscale modeling approach for thermal buckling analysis of nanocomposite curved structure”, *Adv. Nano Res.*, **7**(3), 181.  
<http://doi.org/10.12989/anr.2023.7.3.181>.
- Peng, Ch., Liu, H.C., Wu, M., Han, L. and Wang, Zh. (2023), “A sensitive electrochemical sensor for detection of methyl-testosterone as a doping agent in sports by CeO<sub>2</sub>/CNTs nanocomposite”, *Int. J. Electrochem. Sci.*, **18**, 25-30.  
<https://doi.org/10.1016/j.ijoes.2023.01.014>.
- Taherifar, R., Zareei, S.A., Rabani Bidgoli, M. and Kolahchi, R. (2021), “Application of differential quadrature and Newmark methods for dynamic response in pad concrete foundation covered by piezoelectric layer”, *J. Comput. Appl. Math.*, **382**, 113075. <https://doi.org/10.1016/j.cam.2020.113075>.
- Thai, H.T. and Vo, T.P. (2012), “A nonlocal sinusoidal shear deformation beam theory with application to bending, buckling, and vibration of nanobeams”, *Int. J. Eng. Sci.*, **54**, 58-66.  
<https://doi.org/10.1016/j.ijengsci.2012.01.009>.
- Thai, H.T. (2012), “A nonlocal beam theory for bending, buckling, and vibration of nanobeams”, *Int. J. Eng. Sci.*, **52**, 56-64.  
<https://doi.org/10.1016/j.ijengsci.2011.11.011>
- Taherifar, R., Zareei, S.A., Rabani Bidgoli, M. and Kolahchi, R. (2020), “Seismic analysis in pad concrete foundation reinforced by nanoparticles covered by smart layer utilizing plate higher order theory”, *Steel Compos. Struct.*, **37**(1), 99-115,  
<http://doi.org/10.12989/scs.2020.37.1.099>.
- Wang, W., Jin, Y., Mu, Y., Zhang, M. and Du, J. (2023), “A novel tubular structure with negative Poisson's ratio based on gyroid-type triply periodic minimal surfaces”, *Virtual Phys. Prototyp.*, **18**(1), e2203701.  
<https://doi.org/10.1080/17452759.2023.2203701>
- Wuite, J. and Adali, S. (2005), “Deflection and stress behaviour of nanocomposite reinforced beams using a multiscale analysis”, *Compos. Struct.*, **71**, 388-396.  
<https://doi.org/10.1016/j.compstruct.2005.09.011>.
- Yang, L. (2023), “Challenges and recent progress in carbon-based nanocomposites for sportswear and sensing applications”, *Mater. Res. Exp.*, **10**, 052001.  
<https://doi.org/10.1088/2053-1591/accf64>.
- Zamanian, M., Kolahchi, R. and Rabani Bidgoli, M. (2017), “Agglomeration effects on the buckling behaviour of embedded concrete beams reinforced with SiO<sub>2</sub> nano-particles”, *Wind Struct.*, **24**(1), 43-57.  
<http://doi.org/10.12989/was.2017.24.1.043>.